

# An optimized remote sensing recognition approach for straw burning in Henan Province, China

Y. Lin <sup>1,2</sup>, Y. Rong <sup>1</sup>, J. Yu <sup>1,2,\*</sup>, H.C. Zhang <sup>3</sup>, L. Li <sup>1</sup>

<sup>1</sup>College of Surveying, Mapping and Geo-information, Tongji University, Shanghai, China - (linyi, ronv\_228, lilang)@tongji.edu.cn

<sup>2</sup>Research Center of Remote Sensing & Spatial Information Technology, Shanghai, China -2011\_jieyu@tongji.edu.cn

<sup>3</sup>Chinese Academy of Surveying and Mapping, Beijing, China- zhanghc@casm.ac.cn

## Commission III, WG III/1

**KEY WORDS:** Satellite Remote Sensing, Optimised Threshold Determination Method, Henan Province, Straw Burning, Fire Point Recognition.

### ABSTRACT:

In the paper, Henan Province with prevalent straw burning was taken as the study case. Aimed at remote sensing recognition of the straw burning fire points in a large-scale area with complex terrain and climate conditions, an optimized recognition strategy of straw burning was proposed based on the MOD021KM data. In our new recognition strategy, the threshold determination method was optimized by systematic statistical analysis of spectral features. Then the non-straw burning fire points were eliminated by extracting the agricultural land from MCD12Q1 image. Thus, the true straw-burning fire points were determined. The results showed that the recognition accuracy of straw burning fire points was effectively improved by optimized threshold determination method.

## 1. INTRODUCTION

The phenomenon of centralized burning of straw widely exists in rural areas and the suburbs of large and medium-sized cities in China (Hu et al., 2012). According to statistics, about 160 million tons of straw are burned outdoors every year, accounting for more than a quarter of the total output of straw in the whole year in China (Cao et al., 2006). The harmful gases and particles produced by straw burning have become one of the pollution sources of smog, which has a great impact on the atmosphere, the environment and human health (He et al., 2007; Stavrou et al., 2016; Jiang et al., 2019). Therefore, it is imperative to extract and monitor the straw burning phenomenon accurately and effectively.

MODIS remote sensing (RS) images have a large coverage area and short repeat cycle, which are suitable for large-scale macro monitoring. The application of MODIS images to large-scale fire monitoring is an important aspect of its application. Its multi-band data can reflect the land, cloud boundary and other characteristic information at the same time (Madhavan et al., 2021). It can detect much smaller and more fire points (minimum area up to 50 m<sup>2</sup>) by both higher temporal resolution and temperature point sensitivity than Meteorological Satellite (Teo, 2011), which greatly makes up for the shortcomings of the original monitoring methods based on field inspection.

At present, researchers have carried out extensive research in this field (Giglio et al., 2003; Zhang et al., 2005a; Wang et al., 2008). Flannigan et al. (1986) put forward an absolute threshold model for the environmental characteristics of North American forest areas. Zhou et al. (2006) proposed an improved algorithm for adjacent background pixels. Shao et al. (2012) adjusted the threshold conditions by adding a correction coefficient. By

calculating the cloud area, Zhou et al. (2017) reduced the impact of cloud in the process of straw burning monitoring. However, the previous methods are hardly applied to the complex terrain and climate conditions.

The main areas of straw burning in China are distributed in Hebei, Shandong, Henan, Anhui and other places (Wang et al., 2011). Among them, Henan Province is surrounded by mountains on three sides, with large undulating terrain, complex and diverse climate conditions (Xue, 2020). These characteristics make it more difficult to monitor the phenomenon of straw burning in this area. Hence, in this study Henan Province was regarded as the study area. Based on the MODIS series data, through a series of statistical analysis of spectral characteristics and threshold adjustment, an optimized recognition strategy for straw burning was proposed. Then non-straw burning fire points which were not on the agricultural land were eliminated. Finally, the accurate recognition of straw burning fire points during summer and autumn harvest in Henan Province was performed.

## 2. STUDY AREA AND DATA SOURCES

### 2.1 Study Area

Henan Province, with a total area of about 167000 km<sup>2</sup> and the largest grain output in China, is a typical agricultural province (Figure 1). The province is located in the north temperate zone, and its accumulated temperature conditions can meet the requirement of two crops a year. The staple food crops are wheat and corn, whose harvest time is mainly concentrated in June and early October of each year. During this period, a large amount of crop straw can cause severe burning (Zhu et al., 2016).

\* Corresponding Author

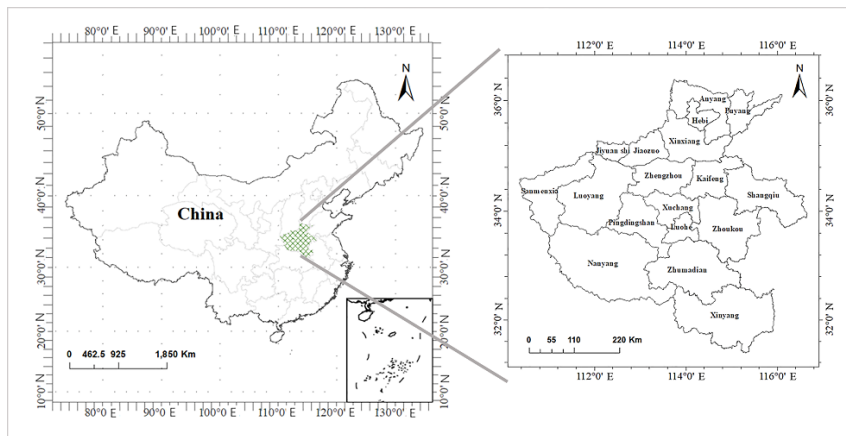


Figure 1. Study area

## 2.2 Data Sources

MODIS sensor has outstanding advantages in large-scale regional fire monitoring because of its both high temporal and hyperspectral resolution, moderate spatial resolution and large image coverage (Gao et al., 2005; He et al., 2008).

In this study, various MODIS data (Table 1) were collected and applied (available at <http://ladweb.modaps.eosdis.nasa.gov>), including: (1) MOD021KM data for extracting the fire point information of straw burning during summer and autumn harvest in Henan Province. (2) MCD12Q1 data for agricultural land extraction. The land cover data set includes 17 types of land cover with a spatial resolution of 500 m, and contains five classification schemes for land cover types (Hou et al., 2019). Different digital number (DN) values on the image represent different types of land features, and the corresponding pixels with the DN value of 12 are agricultural land pixels. (3) MOD14 data is obtained by the sensors on Terra satellite, including the thermal anomaly data caused by biomass combustion and fire, with a spatial resolution of 1 km. There are 10 different DN values in the data. Among them, pixels with DN values of 7, 8 and 9 represent fire points (Csiszar et al., 2006).

In addition, the daily report of environmental satellite monitoring of straw burning (DR) is produced by the satellite application center of the Ministry of Environmental Protection of China. The DR makes detailed statistics on the distribution and quantity of straw burning fire points in the whole country on that day. In this study, MOD14 thermal anomaly data and DR were used as auxiliary data to verify the experimental results.

RS data	Type	Band number	Spatial resolution(m)
MOD021KM	MODIS1B data product	1	250
		2	250
		18	1000
		21	1000
		26	1000
MCD12Q1	MODIS Level 3 land cover type data product	31	1000
	MODIS Level 2 surface heat anomaly data product		500
MOD14	MODIS Level 2 surface heat anomaly data product		1000

Table 1. Specific information about the RS data.

## 3. RESEARCH METHOD

The purpose of fire point detection is to extract the open fire pixels during satellite transit, which is called fire point. This study proposed an optimized recognition strategy of straw burning (Figure 2) based on the MODIS images. In this strategy, the threshold method was constructed by a series of systematic statistical analysis of spectral features. Based on this, the decision tree classification model was used to process the RS image data of MOD021KM to extract the cloud and fire points. Then MCD12Q1 image data was utilized to extract the agricultural land, and the non-straw burning fire points were eliminated based on the agricultural land. Finally, the straw burning fire points were recognized.

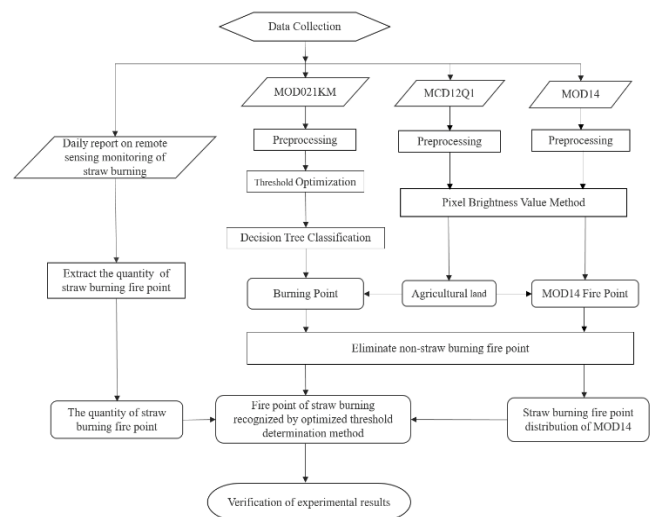


Figure 2. Workflow of the optimized threshold determination method.

### 3.1 Image Pre-processing

RS image data pre-processing mainly includes geometric correction, reflectivity and emissivity calculation, brightness temperature conversion, image clipping, etc. In addition, in order to facilitate the use of images with inconsistent spatial resolution, they were all resampled to 250m (Zhang, 2016).

When the MODIS detector is used to observe the earth, the RS image will be distorted due to the influence of the sensor's own characteristics, earth-curvature, terrain undulation and sensor jitter during operation. Therefore, it is necessary to correct it. The correction process mainly includes eliminating bowtie effect and GLT (Geographic lookup table) geometric correction (Wolf et al., 1998; Liu et al., 2004; Du et al., 2009; Zhang et al., 2013). MODIS series data are stored with 16 signed integers after calibration. They must be converted into available values for practical application. In this study, the reflectivity of band 1, 2, 18, 26 and the emissivity of band 21, 31 were calculated for cloud recognition and subsequent brightness temperature conversion.

$$R = R_{scale} * (SI - R_{offset}) \quad (1)$$

$$\varepsilon = \varepsilon_{scale} * (SI - \varepsilon_{offset}) \quad (2)$$

where  $R$  = reflectivity  
 $R_{scale}$  = calibration gain coefficient  
 $R_{offset}$  = reflection calibration offset  
 $\varepsilon$  = emissivity  
 $\varepsilon_{scale}$  = calibration gain coefficient  
 $\varepsilon_{offset}$  = radiometric calibration offset  
 $SI$  = effective count value of image

Each parameter value can be obtained from the corresponding band data attribute of MODIS HDF data set (Zhang, 2016). When using the threshold method to extract fire points, the brightness temperature of the surface is one of the most important features (Zhang et al., 2005b). According to the emissivity of each radiation band, the brightness temperature value of the corresponding pixel is calculated.

$$T = \frac{hc}{k\lambda} \frac{1}{\ln(\frac{2hc^2}{\lambda^5 \varepsilon} + 1)} \quad (3)$$

where  $T$  = surface brightness temperature value  
 $h$  = the Planck constant  
 $c$  = the speed of light  
 $\lambda$  = the central wavelength of the wave band  
 $k$  = the Boltzmann constant

### 3.2 Threshold Optimization

The threshold condition is the key factor when using the threshold method to extract the fire point. The original threshold method uses a uniform threshold standard to monitor global fire points (He et al., 2008). Due to the mutual influence of different regions, changeable environments and complex climate conditions, the fire threshold should be set according to the specific situation. Combined with a large number of MODIS images in Henan Province, the original threshold conditions were adjusted through many experiments and statistics to analyse the spectral characteristics of straw burning fire points.

**3.2.1 Cloud identification:** In the mid-infrared and near-infrared bands, with the increase of wavelength, the reflectivity of cloud will gradually decrease. While in the visible band, the reflectivity of cloud is higher (Du et al., 2009). Therefore, the reflectivity threshold of visible band 1 can be set as a condition to distinguish cloud body. In band 26, the water vapor has been completely absorbed, so it can hardly receive the reflection spectrum from the middle and low clouds and the ground, but can completely receive the reflection spectrum from the high clouds. Therefore, the high clouds can also be identified by

setting a threshold for the reflectivity of band 26. Zhang (2016) made statistical analysis on the spectral characteristics of a large number of clouds data, and concluded that the reflectivity of cloud in band 1 ( $R_1$ ) and band 26 ( $R_{26}$ ) mostly meet  $R_1 > 0.2$ ,  $R_{26} > 0.02$ . Referring to the results, the parameters were finetuned and statistically analyzed through carrying out several experiments using the real data of Henan Province. The results showed that the reflectivity of cloud in visible band 1 was greater than 0.25 in Henan Province. Therefore, the pixels satisfying the following conditions can be recognized as clouds first:

$$R_1 > 0.25 \quad (4)$$

$$R_{26} > 0.02 \quad (5)$$

In addition, due to the influence of atmospheric water vapor, the spectral characteristics of clouds in band 18 are distributed in the form of absorption valleys. When there is lower cloud, the surface humidity reflection cannot reach the receiver of band 18. This will make the corresponding reflectivity appear virtually high, so that its value will normally be greater or equal to the reflectivity of the near-infrared band in general. Therefore, the normalized cloud detection index ( $CDI$ ) of the unified cloud was calculated by using the reflectance of band 18 and band 2. The processing can not only be used to identify clouds, the errors of atmospheric radiation and instrument system characteristics can also be eliminated (Teo, 2011).

$$CDI = \frac{\rho_{0.66\mu m} - \rho_{0.936\mu m}}{\rho_{0.66\mu m} + \rho_{0.936\mu m}} \quad (6)$$

where  $\rho$  = the reflectivity of corresponding band

When  $CDI > 0$ , the pixels were considered as cloud. For specific band data, the above equation becomes:

$$\frac{R_{18} - R_2}{R_{18} + R_2} > 0 \quad (7)$$

where  $R_{18}$ ,  $R_2$  = reflectivity of band 18 and band 2 respectively.

**3.2.2 Fire point recognition:** At normal atmospheric temperature, the radiation range of surface soil temperature is concentrated in the far-infrared channel, but when there are fire points, the radiation peak is mainly concentrated in the mid-infrared band. According to Wien's Displacement Law, the higher the fire temperature is, the shorter the radiation peak will be. Therefore, the high temperature points on the ground can be extracted by setting a certain threshold value for the brightness temperature values of thermal infrared band 21 and 31 ( $T_{21} > h_{21}$ , and  $T_{31} > h_{31}$ , where  $T_{21}$  and  $T_{31}$  are the brightness temperature value of band 21 and band 31, respectively). The results of Wang et al. (2008) showed that the brightness temperature of non-fire point pixels in band 21 is less than 340 in China. Kaufman et al. (1989) pointed out that setting a threshold of 250 for the brightness temperature value of band 31 can eliminate the influence of cloud reflection on the saturation of high temperature band. However, in the actual test using a large number of images in Henan Province, these thresholds are not effective for fire point recognition and need to be adjusted. Generally, when the brightness temperature of mid-infrared data in the study area is counted, it will be found that the fire point pixels only account for a small part of its high temperature (Wang et al., 2011). Therefore, the threshold  $h_{21}$ , and  $h_{31}$  can be set by calculating the percentage of each bright

temperature value in the total number of pixels of the actual data. In this paper, brightness temperature values  $h_{21}=309$ , and  $h_{31}=285$ , which account for 5% of the total pixels, are selected as corresponding thresholds (He et al., 2008). Then the above judgement changes to  $T_{21} > 309$ , and  $T_{31} > 285$ . This adjustment can not only ensure the credibility of the fire points, but also improve the number of fire points fulfilling the absolute threshold. It is convenient for the next step of judgment and recognition.

Among the recognized high-temperature points, there is also high-temperature ground besides the burning point. Their radiation is stronger in the far-infrared band than in the fire point. To eliminate the influence of ground high temperature points, the difference between mid-infrared band 21 and far-infrared band 31 can be used to further select the extracted high temperature points (Eva et al., 1996; Zhou et al., 2014). Combined with the actual data, the difference of brightness temperature values of fire points in band 21 and band 31 was counted respectively. Wang et al. (2008) noted that the difference between the recognized fire points in the two bands is more than 14.5.

To further improve the accuracy of the recognition of the burning point of straw in Henan Province, the threshold, as the Formula (8), was set through a large number of experiments and statistical analysis:

$$T_{21} - T_{31} > 14.95 \quad (8)$$

### 3.3 Accuracy Assessment

To assess the accuracy of fire point recognition comprehensively, both quantity and spatial location were verified respectively. The quantitative accuracy was assessed in terms of the correct number of recognized fire points on RS data. Based on the statistical data issued by Henan Environmental Protection Department, the accuracy which is the ratio of the total number of correctly monitored thermal abnormal points to the total number of recognized thermal abnormal points was calculated to assess the recognition results (Yang et al., 2009). Additionally, other two widely utilized methods (original threshold method and pixel brightness value method) were applied as well to make a quantitative comparison experiment (Zhang, 2016; Yang et al., 2009). On the other hand, to assess the spatial recognition accuracy, the accuracy of the spatial position was verified by comparing with the fire point position of MOD14 (Wang et al., 2008).

## 4. EXPERIMENTAL RESULTS AND ANALYSIS

### 4.1 Fire Point of Straw Burning Recognition

In this study, the fire point on agricultural land is regarded as the fire point of straw burning, so it is necessary to extract

agricultural land in order to remove the interference of forest fire, artificial building heat and other non-straw burning fire points. Different DN values on the MCD12Q1 image represent different types of ground objects. Among them, the corresponding pixels with a DN value of 12 can be extracted by the pixel brightness value method to extract agricultural land in Henan Province. As an example, Figure 3(a) shows the results in 2014. Then the fire points of straw burning were recognized through the intersection of the extracted burning points and the agricultural land. Figure 3(b) shows the distribution of straw burning points on June 11, 2014. It can be seen that the total number of fire points recognized was 22, and the fire points are mainly distributed in the northern regions of Henan Province. Among them, Puyang has the most fire points reaching 11. It accounts for 50% of the total number of fire points recognized.

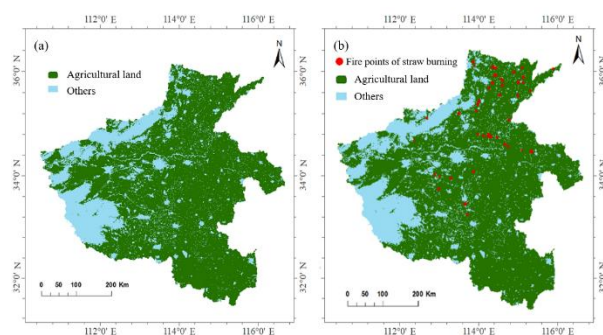


**Figure 3.** Recognition results of straw burning points: (a) agricultural land in 2014; (b) fire points of straw burning on June 11, 2014.

### 4.2 Accuracy Assessment Results

The MODIS data during the harvest period (May-June and September-October) in Henan Province were selected for the experiment. Limited by the length of the article, only four images of MOD021KM with a large number of fire points on June 11, 2014, October 7, 2014, June 9, 2015 and October 1, 2015 were selected for accuracy verification according to the accuracy assessment method of 3.3. Among them, the final results of June 11, 2014 were utilized to assess the quantitative accuracy. While other three data were applied to compare and analyse the spatial location.

**4.2.1 Quantity Assessment of Fire Points:** The DR issued by the official was used as a reference to verify the quantitative information of straw burning fire points recognized. Meanwhile, the fire points recognized by the original threshold method and pixel brightness value method were also compared with the results. The comparison and statistical results are shown in Table 2 and Figure 4.

City	Official issued data	Original Threshold Method	Pixel Brightness Value Method	Optimized Threshold Determination Method
Anyang	1	0	0	0
Puyang	11	13	5	11
Pingdingshan	1	5	0	0
Luohe	2	4	1	2
Zhoukou	2	2	1	2

Shangqiu	1	5	5	2
Xuchang	1	5	1	1
Zhumadian	1	3	1	1
Xinyang	4	2	3	3
Total	24	34	17	22
Accuracy	—	61.76%	76.47%	95.45%

**Table 2.** Statistical table of verification results of quantity of straw burning fire points on June 11, 2014.

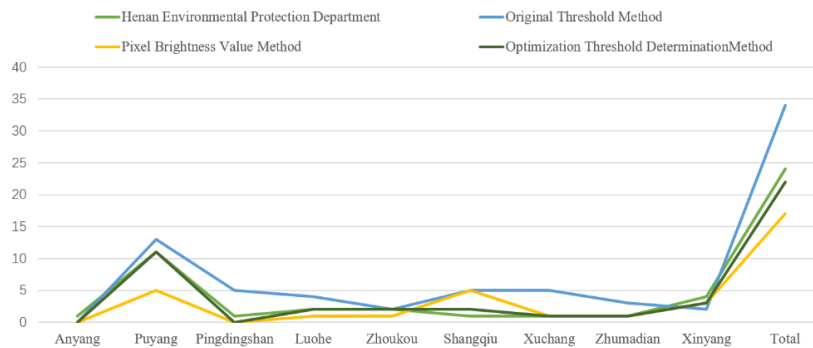


**Figure 4.** Comparison and statistics of the number of recognized straw burning fire points on June 11, 2014.

It can be seen from Figure 4 that the total number of fire points in the DR is 24, and the total number of fire points recognized by the original threshold method is 34. According to the analysis of the fire point's location, 21 real fire points were found, 3 were missed and 10 were misjudged. The accuracy was 61.76%. The total number of fire points recognized by pixel brightness value method was 17, 13 real fire points among which were recognized, 4 false fire points and 11 missed fire points were recognized. The accuracy was 76.47%. While the total number of fire points recognized by the optimized threshold determination method was 22, of which 21 were real fire points, 3 were missed and 1 was misjudged. Its accuracy was 95.45%.

The same method was used to compare and verify the fire points extracted from other dates (Figure 5). The statistical results

showed that the accuracy of fire point recognition by the optimized threshold determination method is all above 90%, which indicates its highest recognition accuracy. Specifically, the accuracy of the original threshold method and the pixel brightness value method was 60.25% and 81.58% on October 7, 2014, while the optimized threshold determination method was 91.11%. On June 9, 2015, the accuracy of the original threshold method was 58.13%, the pixel brightness value method was 71.43%, and the optimized threshold determination method was 95.24%. On October 1, 2015, the accuracy of the original threshold method was 63.49%, the pixel brightness value method was 85.71%, and the optimized threshold determination method was 96.06%.

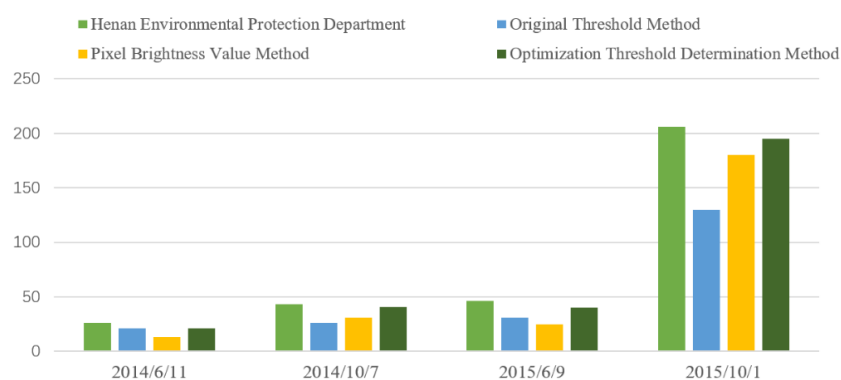


**Figure 5.** Statistics of the number of fire spots correctly recognized on June 11, 2014, October 7, 2014, June 9, 2015 and October 1, 2015.

Compared with the original threshold method, the optimized threshold determination method improved the recognition accuracy of fire point by an average of 30%, which indicates that the optimized threshold determination method is more suitable for fire point recognition in Henan Province. According to the extraction result of the pixel brightness value method, the original thermal anomaly image data of MODIS are limited by its processing method, and there are certain omissions and misjudgments (Wang et al., 2008). In contrast, the optimized threshold determination method had a higher accuracy of straw burning fire recognition.

**4.2.2 Spatial Location Verification of the Fire Points:** MOD14 image is a MODIS secondary surface heat anomaly data product, including thermal anomaly data generated by biomass combustion and fire. Wang et al. (2008) and Yang et al. (2009) showed that the spatial location of fire points extracted from MOD14 thermal abnormal images had a certain reliability. Meanwhile, affected by the lack of ground fire point survey data, the spatial location accuracy of fire points recognized by the optimized threshold determination method was verified by comparing with the distribution of fire points recognized from MOD14 images (Figure 6).

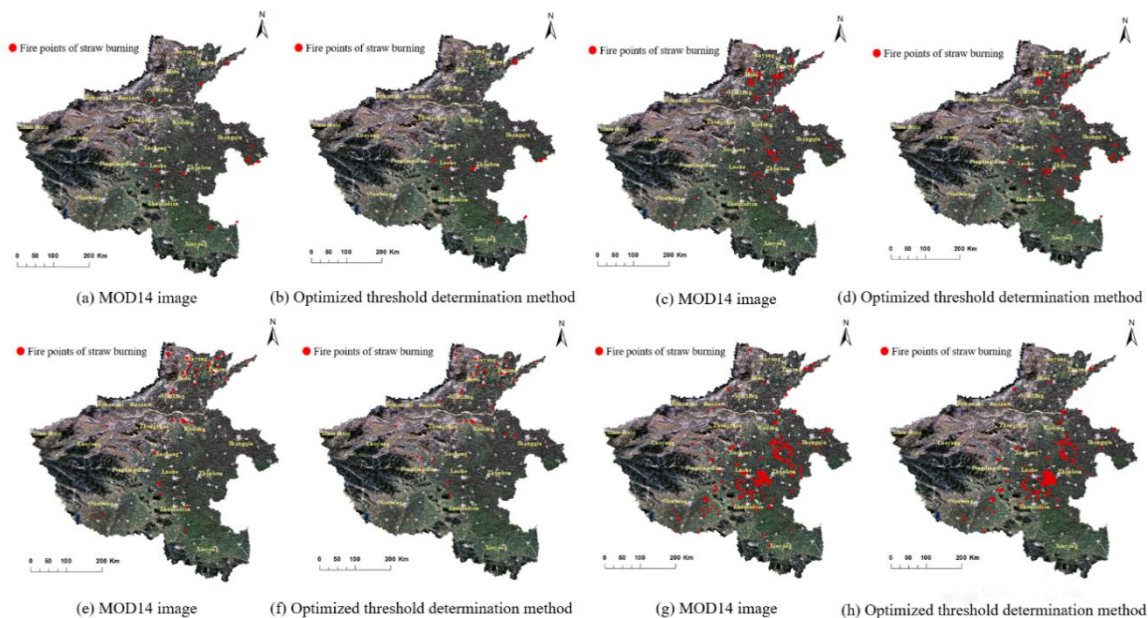


**Figure 6.** Distribution comparison of fire points of straw burning on June 11, 2014: (a), (b); October 7, 2014: (c), (d); June 9, 2015: (e), (f); and October 1, 2015: (g), (h).

According to statistics, on 11 June, 2014, 7 October, 2014, 9 June, 2015 and 1 October, 2015, there are 13, 31, 25 and 180 fire points of straw burning recognized by the optimized threshold determination method have consistent coordinates with the MOD14 image, respectively. It means that the spatial location of the real fire points recognized by both of them has a good consistency. The results further proved the reliability of the location distribution of the straw burning fire points recognized by the method in this study.

## 5. CONCLUSION

In this study, an optimized recognition strategy of straw burning was proposed based on MOD021KM data. This threshold method was constructed by a series of systematic statistical analysis of spectral features and reasonable adjustment of the threshold values of many thermal channels of MODIS products. And the non-straw burning fire points in Henan Province were eliminated by extracting the agricultural land from MCD12Q1 image. At the same time, to assess the quantity and the spatial location of the straw burning fire points recognized by the proposed method, the recognized fire points on 11 June, 2014, 7 October, 2014, 9 June, 2015 and 1 October, 2015 were respectively compared with the fire point information reflected

by the DR issued by Henan Environmental Protection Department and the MOD14 thermal abnormality imaging. The results show that the optimized threshold determination method has the highest accuracy reaching 95.45%, which is 33.69% and 18.98% higher than the original threshold method and the pixel brightness value method, respectively. Meanwhile, the spatial distribution of the recognized fire points is also reliable. This means the recognition accuracy of straw burning fire points in Henan Province was effectively improved by the optimized threshold determination method. This method made up for the deficiency of the ground manual inspection-based environmental monitoring method, and provided a reference for the follow-up related research.

In summary, this study has made some significant exploration in monitoring the phenomenon of straw burning in Henan Province with MODIS satellite data. However, due to the limitation of the spatial resolution, only the spatial distribution of burning points was determined. The accurate burning area cannot be studied. Therefore, in the follow-up study, MODIS data can be used to preliminarily locate the fire point, and then the burned area can be extracted by combining with high spatial resolution RS data such as Landsat 8 and Sentinel images. At the same time, it can also be used to verify the fire point and further improve the accuracy of fire point recognition.

## ACKNOWLEDGEMENTS

The study was financially supported by National Key R&D Program of China (Grant number: 2018YFB0505400), the Key Laboratory of Surveying and Mapping Science and Geospatial Information Technology, Ministry of Natural Resources, Beijing, China (No. 2020-2-3).

## REFERENCES

- Hu, M., Qi, S.H., Shu, X.B., Chen, L.F., 2012. Monitoring fire from crop residues burning with MODIS data in North China Plain. *J. Geogr. Inf. Sci.*, 10(6):802-807. doi.org/10.3969/j.issn.1560-8999.2008.06.021.
- Cao, G.L., Zhang, X.Y., Zheng, F.C., Wang, Y.Q., 2006. Estimating the quantity of crop residues burnt in open field in China. *Resour. Sci.*, 28(1):9-13. doi.org/10.1007/s11442-006-0415-5.
- Csiszar, I.A., Morisette, J.T., Giglio, L., 2006. Validation of active fire detection from moderate-resolution satellite sensors: the MODIS example in northern Eurasia. *IEEE Trans. Geosci. Remote Sens.*, 44(7):p.1757-1764. doi.org/10.1109/tgrs.2006.875941.
- Du, Q.S., Liu, Z.P., Wang, X.S., Ma, N., 2009. Method for MODIS data pre-processing based on ENVI. *Geo. Spat. Inf.*, 7(04):98-100. doi.org/10.3969/j.issn.1672-4623.2009.04.033.
- Eva, H., Flasse, S., 1996. Contextual and multiple-threshold algorithms for regional active fire detection with AVHRR data. *Remote Sens. Rev.*, 14(4):333-351. doi.org/10.1080/02757259609532324.
- Flannigan, M.D., Haar, T.H.V., 1986. Forest fire monitoring using NOAA satellite AVHRR. *Can. J. For. Res.*, 16(5):975-982. doi.org/10.1139/x86-171.
- Gao, M.F., Tan, H., Liu, S.C., 2005. A study of forest fire detection based on MODIS data. *Remote Sens. Land. Resour.*, (02):60-63+84. doi.org/10.6046/gtzyyg.2005.02.14.
- Giglio, L., Descloitres, J., Justice, C.O., Kaufman, Y.J., 2003. An enhanced contextual fire detection algorithm for MODIS. *Remote Sens. Environ.*, 87(2):273-282. doi.org/10.1016/S0034-4257(03)00184-6.
- He, L.M., Wang, W.J., Wang, Q., Wei, B., Li, Q., Wang, C.Z., Liu, X.M., 2007. Evaluation of the agricultural residues burning reduction in China. *Environ. Monit. China*, (01):42-50. doi.org/10.3969/j.issn.1002-6002.2007.01.013.
- He, Q.J., Liu, C., 2008. Improved algorithm of self-adaptive fire detection for MODIS data. *Natl. Remote Sens. Bull.*, (03):448-453. doi.org/10.1016/S1001-0742(08)62079-3.
- Hou, W., Hou, X.Y., 2019. Consistency of the multiple remote sensing-based land use and land cover classification products in the global coastal zones. *J. Geogr. Inf. Sci.*, 21(07):1061-1073.
- Jiang, M.H., Huo, Y.Q., Huang, K., Li, M., 2019. Way forward for straw burning pollution research: a bibliometric analysis during 1972–2016. *Environ. Sci. Pollut. Res. Int.*, 26(14):13948-13962. doi.org/10.1007/s11356-019-04768-0.
- Kaufman, Y.J., Tucker, C.J., Fung, I.Y., 1989. Remote sensing of biomass burning in the tropics. *J. Geophys. Res.: Atmos.*, 95(D7):371-399. doi.org/10.1007/978-3-642-75395-4\_16.
- Liu, L.M., Yan, J.J., 2004. Fire detection based on EOS MODIS data. *Geomatics Inf. Sci. Wuhan Univ.*, (01):55-57+94-95.
- Madhavan, S., Sun, J., Xiong, X., 2021. Sensor calibration impacts on dust detection based on MODIS and VIIRS thermal emissive bands. *Adv. Space. Res.*, 67(10):3059-3071. doi.org/10.1016/j.asr.2021.02.035.
- Shao, W.W., Yang, Z., Zhou, B., 2012. Improvement of remote sensing identifying methods of crop residue burning based on moderate-resolution imaging spectroradiometer data. *Environ. Poll. Control.*, 34(09):38-42. doi.org/10.3969/j.issn.1001-3865.2012.09.009.
- Stavrakou, T., Müller, J.F., Bauwens, M., De Smedt, I., Lerot, C., Van Roozendaal, M., Coheur, P.F., Clerbaux, C., Boersma, K.F., Van Der A, R., Song, Y., 2016. Substantial underestimation of post-harvest burning emissions in the North China Plain revealed by multi-species space observations. *Sci. Rep.*, 6(1):1-11. doi.org/10.1038/srep32307.
- Teo, T.A., 2011. Bias compensation in a rigorous sensor model and rational function model for high-resolution satellite images. *Photogramm. Eng. Rem. S.*, 77(12):1211-1220. doi.org/10.14358/PERS.77.12.1211
- Wang, L., Tian, Q.J., Bao, Y., 2011. Straw-burning fire detection using HJ-1B IRS data. *Sci. Geogr. Sin.*, 31(06):661-667. doi.org/10.1155/2011/531540.
- Wang, Z.F., Chen, L.F., Gu, X.F., 2008. Monitoring of crop residue burning in North China on the basis of MODIS data. *Remote Sens. Tech. Appl.*, 23(6):611-617. doi.org/CNKI:SUN:YGJS.0.2008-06-000.
- Wolf, O.E., Roy, D.P., Vermote, E., 1998. MODIS land data storage, gridding, and compositing methodology: level 2 grid. *IEEE Trans. Geosci. Remote Sens.*, 36(4):1324-1338. doi.org/10.1109/36.701082 .Source: IEEE Xplore.
- Xue, M.H., 2020. Spatio-temporal distribution characteristics of drought in Henan and Shandong Provinces based on MODIS. *J. Subtrop. Resour. Environ.*, 15(2):81-87.
- Yang, S.R., Li, H., Yu, T., Li, J.G., Wang, Z.F., 2009. Principle of identifying crop straw fire based on MODIS and its algorithm implementation using IDL language. *Remote Sens. Inf.*, (2):91-97. doi.org/10.3969/j.issn.1000-3177.2009.02.018.
- Zhang, H.X., 2016. Research on the remote sensed monitoring in crop straw burning fire based on MODIS in Jiangxi Province. East China University of Technology, Jiangxi, China.
- Zhang, S.Y., Li, D.K., Jing, Y.G., 2005a. Application of “3S” technology in remote sense monitoring for stalk burning in Guanzhong Region. *Adm. Tech. Environ. Monit.*, 17(2):17-20. doi.org/
- Zhang, S.Y., Li, D.K., Li, X.M., Jing, Y.G., 2005b. Application of remote sensing data to monitoring straw burning. *Meteorol. Mon.*, 31(9):83-86. doi.org/10.1007/s10971-005-6694-y.

Zhang, Y., He, Z.W., Xue, D.J., 2013. Pre-processing method of MODIS data. *Geo. spat. Inf.*, 11(03):49-50+4.

Zhou, B., Zhang, X., Han, Y.Y., 2017. Study on the influence of cloud covering on the fire point of straw by satellite remote sensing. *Zhejiang Chem. Ind.*, 48(08):44-47. doi.org/CNKI:SUN:ZJHG.0.2017-08-016.

Zhou, X.C., Wang, X.Q., 2006. Validate and improvement on arithmetic of identifying forest fire based on EOS-MODIS data. *Remote Sens. Tech. Appl.*, 21(3):206-211. doi.org/10.1007/s11769-006-0026-1.

Zhou, Y.B., Han, H., 2014. Research overview of forest fire monitoring based on remote sensing data. *Geomatics Spat. Inf. Tech.*, 37(3):134-136. doi.org/10.3969/j.issn.1672-5867.2014.03.039.

Zhu, S.M., Chen, W.Q., Cheng, D.Q., 2016. Zhao YF. Study on realizable grain production potential in Henan Province. *J. Henan Agric. Univ.*, 050(001):115-121.